

Inclined N₂ Desorption in a Steady-State NO + CO Reaction on Pt(100)

Hideyuki Horino[†] and Tatsuo Matsushima^{*‡}

*Graduate School of Environmental Earth Science, Hokkaido University, Sapporo 060-0810, Japan, and
Surface Reaction Dynamics Laboratory, Catalysis Research Center, Hokkaido University,
Sapporo 001-0021, Japan*

Received: October 22, 2004; In Final Form: December 8, 2004

The angular and velocity distributions of desorbing products N₂ and CO₂ were studied in a steady-state NO + CO reaction on Pt(100). From the observation of the inclined N₂ desorption, a contribution of the intermediate N₂O decomposition pathway was first proposed on this surface. On the other hand, CO₂ desorption collimated along the surface normal.

I. Introduction

The reaction of NO + CO on platinum metals is one of the key processes of three-way catalysts. To continue the catalytic cycle steadily, deposited oxygen and nitrogen must be removed from catalyst surfaces. Oxygen removal has been well studied on platinum, whereas the removal of nitrogen is still not clear.¹ This paper reports the first observation of inclined N₂ desorption in a steady-state CO + NO reaction on a Pt(100) surface, indicating a contribution of the intermediate N₂O decomposition pathway.

A clean Pt(100) surface is reconstructed into a hexagonal form (hex) at 370–400 K. The form is converted into many small domains of the (1×1) form by the adsorption of CO at room temperature or below it.^{2,3} The resultant (1×1) surface is highly active toward NO dissociation.⁴ Kinetic studies at steady-state or well-known oscillation conditions induced by the structure transformation between (1×1) and (hex) are not informative for the surface-nitrogen reactions because of their fast removal.⁵ On the other hand, the angular and velocity distributions of desorbing products can provide information on the product desorption processes even if these are not rate-determining.¹ Recently, Ohno et al. reported that both desorbing N₂ and CO₂ collimated along the surface normal in the explosive NO + CO reaction⁶ under temperature-programmed desorption (TPD) conditions and discussed the possibility of the inclined N₂ desorption along the [011] direction.⁷

II. Experiments

The experiments were carried out in an ultrahigh vacuum apparatus consisting of three chambers separately pumped, i.e., (i) a reaction chamber with LEED-AES, an Ar⁺ gun and a mass spectrometer (MS), (ii) a chopper house with slits and a cross-correlation chopper, and (iii) an analyzer with another MS.⁸ Product molecules desorbing from a sample surface can be detected in the analyzer after passing the two slits, yielding angle-resolved (AR) signals. For time-of-flight measurements,

the flow of products was modulated by the chopper, and their arrival time at the ionizer in the analyzer MS was recorded. The time resolution was 15 μs. The crystal was rotated to change the desorption angle (θ ; polar angle) in the normally directed plane along the [011] direction (Figure 1). The sample surface was cleaned by repeated Ar⁺ bombardments at 2 keV and the surface temperature (T_s) of 1000 K and heating in oxygen at 5×10^{-7} Torr at around $T_s = 850$ K. It was finally annealed to 1100 K, showing the (hex) structure. ¹³C¹⁶O (purity >99% and less than 1% ¹⁸O) (or ¹²C¹⁶O) and ¹⁵N¹⁶O (purity >99%) gases were used without further purification for the selective detection of desorbing products, ¹³C¹⁶O₂, ¹⁵N₂, and ¹⁵N₂¹⁶O. Hereafter, these species are simply designated as CO₂, N₂, and N₂O in the text.

III. Results

A. General Features. The AR signal at $\theta = 0^\circ$ is shown for desorbing CO₂ and N₂ in a steady-state NO + CO reaction versus T_s (Figure 1a). Their desorption was commonly maximized at the normal direction. The reactants CO and NO were introduced in a back-filled type. The AR signal was obtained by MS in the analyzer as the difference between the signal at the desired angle and the signal when the crystal was away from the line-of-sight position. It was negligible below 400 K, and thereupon, it abruptly reached the maximum at 440–500 K and decreased toward zero at 650 K. In the subsequent cooling, the signal became significant at around 460 K and then jumped to a high rate close to the former maximum, dropping to zero at around 380 K. The AR–N₂O signal at $\theta = 0^\circ$ became noticeable only around the maximum reaction rate, yielding the intensity of about 9% of the N₂ signal. Most desorption measurements were conducted at $T_s = 450$ K, where the reaction rate was insensitive to the NO pressure for the pressure ratio of $P_{\text{NO}}/P_{\text{CO}} > 1.5$. The reaction was suppressed at $P_{\text{NO}}/P_{\text{CO}} < 1.5$. In separate TPD measurements, very small N₂O desorption was also observed.⁷

B. Angular and Velocity Distributions. Both CO₂ and N₂ desorption collimated sharply along the surface normal. The CO₂ signal showed a $\cos^7(\theta)$ form (Figure 1b), whereas desorbing N₂ showed shoulders at around $\pm 36^\circ$ off normal. The N₂ signal at $P_{\text{NO}}/P_{\text{CO}} = 3$ (Figure 2a) was approximated as \cos^{12} .

* Corresponding author. E-mail: tatmatsu@cat.hokudai.ac.jp. Fax: +81-11-706-9120.

[†] Graduate School of Environmental Earth Science.

[‡] Surface Reaction Dynamics Laboratory, Catalysis Research Center.

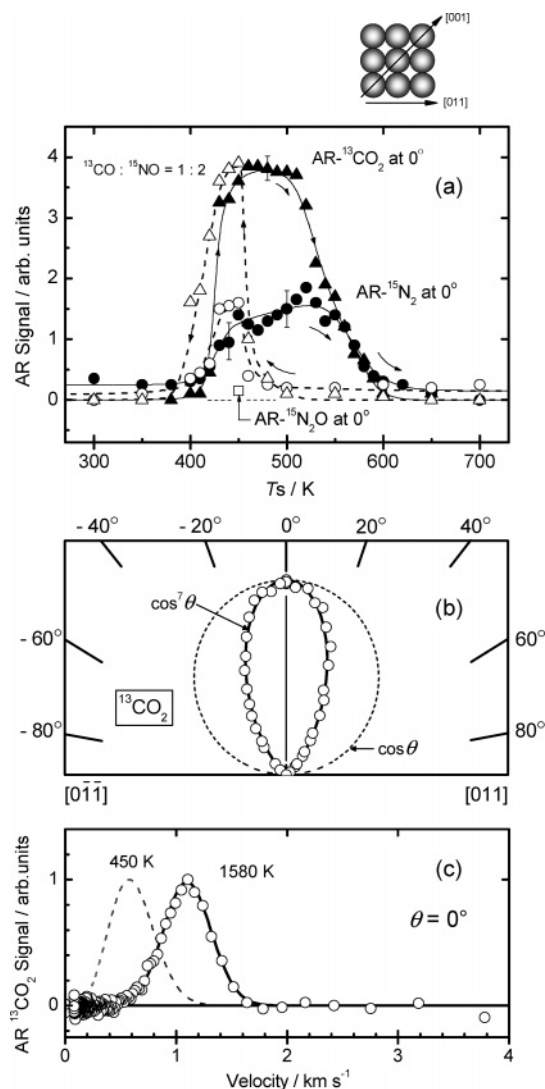


Figure 1. (a) Temperature dependence of the AR signals at $\theta = 0^\circ$ of products in a steady-state ($^{15}\text{NO} + ^{13}\text{CO}$) reaction at 6×10^{-7} Torr of ^{15}NO with a ($^{15}\text{NO}/^{13}\text{CO} = 2$) mixture when the crystal was heated and then cooled. The signals observed in the direction of the increasing surface temperature are designated by closed symbols and those in the downward direction, by open symbols. The signal for N_2O is shown only at the optimum point. (b) Angular and (c) velocity distributions of desorbing $^{13}\text{CO}_2$ at 450 K. The crystal azimuth is shown in the upper part.

(θ) + $0.27 \cos^{60}(\theta \pm 36)$. The shoulder at 36° was alive at about 4 times higher pressure (Figure 3a). The normally directed component became sharper at a higher P_{NO} .

The shoulder showing the inclined desorption was examined from velocity distribution analysis. The velocity curve of desorbing CO_2 at $\theta = 0^\circ$ showed a single component (Figure 1c). The translational temperature, defined as $T_{(E)} = \langle E \rangle / 2k$, was estimated to be 1580 ± 50 K at $\theta = 0^\circ$, where $\langle E \rangle$ denotes the mean kinetic energy and k is the Boltzmann constant. It decreased with increasing the θ value, as is usually observed in repulsive product desorption.¹

The velocity curve of desorbing N_2 involved the thermalized component described by a Maxwell distribution at 350 K (the dotted curve in Figures 2b,c,d and 3b,c). This component came from the background N_2 in the reaction chamber because it was invariant even if the crystal was away from the line-of-sight position. The distribution curve after subtraction of this thermalized component yielded a high translational temperature of about 3000 K, as shown in brackets in the figures. The value

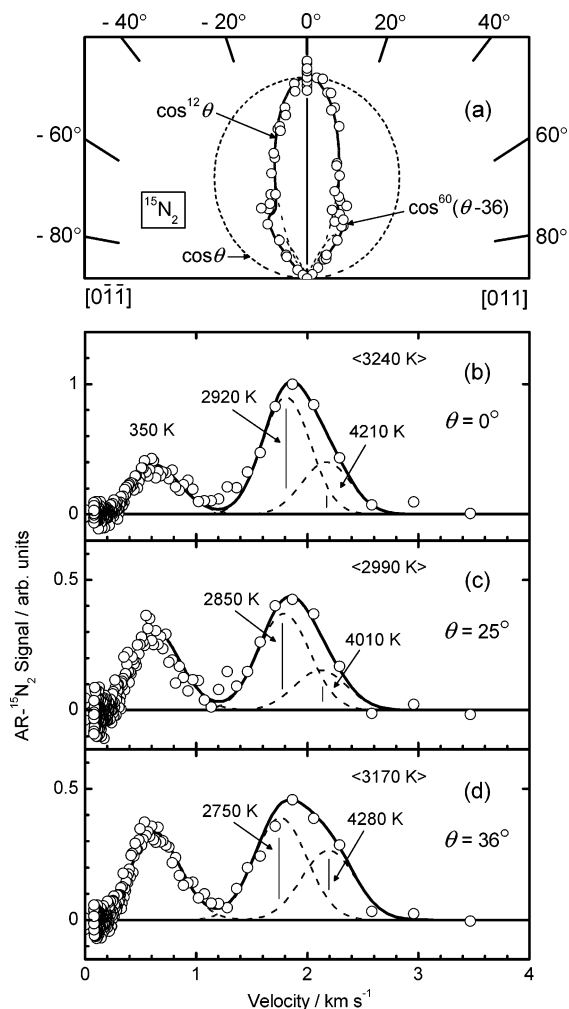


Figure 2. (a) Angular distribution of desorbing $^{15}\text{N}_2$ in the steady-state $^{15}\text{NO} + ^{13}\text{CO}$ reaction with a mixture ($^{15}\text{NO}/^{13}\text{CO} = 3$) at the total pressure of 1.2×10^{-6} Torr and 450 K. Velocity distributions of $^{15}\text{N}_2$ are shown at $\theta =$ (b) 0° , (c) 25° , and (d) 36° . The average kinetic energy of the fast part is indicated in brackets in temperature units. Typical deconvolutions are drawn by broken curves.

was insensitive to the desorption angle, and the fraction of higher velocity components was enhanced at large desorption angles or higher pressures, supporting the inclined desorption.

IV. Discussion

A. Kinetics and Surface-Nitrogen Removal. Hysteresis has frequently been reported in the steady-state $\text{NO} + \text{CO}$ reaction on $\text{Pt}(100)$ and mostly explained by the structural transformation induced by CO(a) and NO(a) between (1×1) and (hex) ;⁵ the reaction rate increases at around 400 K with increasing T_s because of the enhanced CO desorption, which leaves vacant sites available for NO(a) dissociation. The rate reaches a steady value at 420–510 K and decreases quickly above 520 K, where the surface is converted into the (hex) structure. In the subsequent cooling, the rate is recovered at around 450 K where CO or NO can adsorb enough to convert into (1×1) domains. Below 400 K, CO is accumulated into the inhibition level. In other words, NO dissociation and N_2 desorption proceed in the (1×1) form. In fact, in the TPD studies, the structure transformation from (1×1) to (hex) started at about 50 K above the explosive N_2 and CO_2 desorption peaks.⁵ The observed desorption dynamics of N_2 and CO_2 is quite similar to that in the explosive desorption except for the lack of the inclined N_2 desorption and somewhat broader angular distributions of N_2 along the $[001]$ direction.⁷

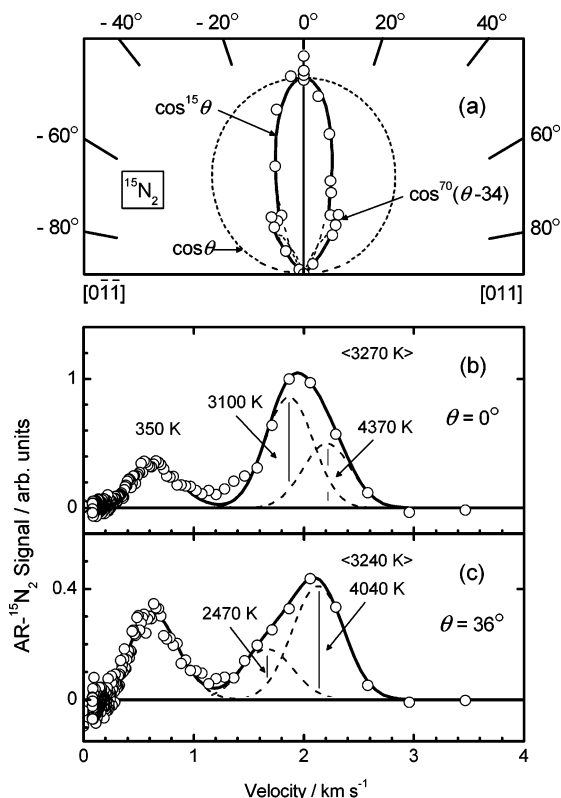


Figure 3. (a) Angular distribution of desorbing $^{15}\text{N}_2$ in the steady-state $^{15}\text{NO} + ^{13}\text{CO}$ reaction with a mixture ($^{15}\text{NO}/^{13}\text{CO} = 3$) at the total pressure of 4×10^{-6} Torr and 450 K. Velocity distributions of $^{15}\text{N}_2$ at $\theta = 0^\circ$ and (c) 36° . The average kinetic energy of the fast part is indicated in brackets in temperature units.

The associative process of $\text{N(a)}, 2\text{N(a)} \rightarrow \text{N}_2(\text{g})$, is very fast on platinum⁹ and emits N_2 along the surface normal.¹ The intermediate formation, $\text{NO(a)} + \text{N(a)} \rightarrow \text{N}_2\text{O(a)}$ is also fast,⁹ and its decomposition emits N_2 in an inclined way. This decomposition is not unreasonable because N_2O dissociates on a stepped Pt(112) even at 300 K.¹⁰ $\text{Pt(100)}(1 \times 1)$ must be more active toward N_2O dissociation, because even NO(a) dissociates. The reaction $\text{CO(a)} + \text{O(a)}$ takes place quickly, emitting CO_2 along the surface normal. The observed energy is close to that in a steady-state $\text{CO} + \text{O}_2$ reaction on platinum surfaces.¹

Recently, a possible intermediate of $-\text{NCO(a)}$ was proposed in a steady-state $\text{NO} + \text{CO}$ reaction from infrared reflection spectroscopy work.¹¹ However, the inclined N_2 emission along about 40° off normal was commonly observed in $\text{NO} + \text{CO}$ and $\text{NO} + \text{H}_2$ reactions on Pd(110) , indicating no direct contribution to N_2 emission from $-\text{NCO(a)}$.¹²

B. Velocity Analysis. To examine the insensitive energy of the fast N_2 component, the velocity distribution was further analyzed. The hyperthermal kinetic energy of desorbing products usually decreases with increasing shift from the collimation angle.¹ On the other hand, the energy of desorbing N_2 noticeably increased from the surface normal to around 40° . Thus, the velocity distribution curve was deconvoluted into *two* components by assuming the modified Maxwellian form,

$$f(v) = v^3 \exp\{-(v - v_0)^2/\alpha^2\}$$

where v is the velocity of the molecule, v_0 is the stream velocity,

and α is the width parameter. The deconvolution was performed in the way reported previously.¹³ The resultant $T_{(E)}$ value for each component is shown in Figures 2 and 3. The faster one showed 4290 ± 100 K at $\theta = 0^\circ$ and 4160 ± 200 K at $\theta = 36^\circ$. The slower one yielded 3010 ± 100 and 2610 ± 200 K at $\theta = 0^\circ$ and 36° , respectively. The fraction of the faster component increased at around 36° and its translational temperature remained invariant, consistent with the presence of the inclined desorption component. The derived fitting curves show a noticeable shift from the observed values in the velocity range of $1.2\text{--}1.5$ km s^{-1} . A better fitting was found when *three* fast components were considered. However, a unique deconvolution became difficult because of many (six) parameters although the fraction and the translational temperature of the fastest component were hardly affected.

These fast components were once proposed to be due to the different vibrational states because their energy differences are close to the excitation energy of the stretching vibration of N_2 , 0.29 eV (or 1700 K);¹⁴ i.e., the fastest component is in the ground vibrational state, and the other is assigned to the first vibrationally excited state. However, the contribution from the products from higher excitation levels cannot be ruled out because of similar energy differences even at higher excitation levels. Experiments with more energy resolutions are highly desired.

In the previous TPD work, the angular distribution of desorbing N_2 was approximated as $\cos^7(\theta)$ in the plane along the $[001]$ direction.⁷ On the other hand, a $\cos^{12-15}(\theta)$ form was found for the normally directed N_2 desorption component along the $[011]$ direction under steady-state conditions. The distribution is broadened in the TPD work. The $\text{Pt(100)}(\text{hex})$ surface is covered by nanometer-size (1×1) domains stabilized by either NO or CO after exposures at low temperatures and these domains may decline from the bulk surface plane yielding broader distributions.^{2,3} On the other hand, the (1×1) domains may grow under steady-state reaction conditions at higher T_s values or higher pressures.

Acknowledgment. H.H. is indebted to the Japan Society for the Promotion of Science for a 2003-2005 fellowship.

References and Notes

- (1) Matsushima, T. *Surf. Sci. Rep.* **2003**, 52, 1.
- (2) Borg, A.; Hilmen, A.-M.; Bergene, E. *Surf. Sci.* **1994**, 306, 10.
- (3) Behm, R. J.; Thiel, P. A.; Norton, P. R.; Ertl, G. *J. Chem. Phys.* **1983**, 78, 7437.
- (4) Rienks, E. D. L.; Bakker, J. W.; Baraldi, A.; Carabineiro, S. A. C.; Lizzit, S.; Weststrate, C. J.; Nieuwenhuys, B. E. *Surf. Sci.* **2002**, 516, 109.
- (5) Imbihl, R.; Ertl, G. *Chem. Rev.* **1995**, 95, 697.
- (6) Lesley, M. W.; Schmidt, L. D. *Surf. Sci.* **1985**, 155, 215.
- (7) Ohno, Y.; Sarawut, P.; Horino, H.; Kobal, I.; Hiratsuka, A.; Matsushima, T. *Chem. Phys. Lett.* **2003**, 373, 161.
- (8) Matsushima, T.; Shobatake, K.; Ohno, Y.; Tabayashi, K. *J. Chem. Phys.* **1992**, 97, 2783.
- (9) Wang, H.; Tobin, R. G.; DiMaggio, C. L.; Fisher, G. B.; Lambert, D. K. *J. Chem. Phys.* **1997**, 107, 9569.
- (10) Burch, R.; Daniells, S. T.; Breen, J. P.; Hu, P. *J. Catal.* **2004**, 224, 252.
- (11) Ozensoy, E.; Goodman, D. W. *Phys. Chem. Chem. Phys.* **2004**, 6, 3765.
- (12) Ma, Y.-S.; Matsushima, T. *J. Phys. Chem. B* **2004**, 109, in press.
- (13) Rzeznicka, I. I.; Ma, Y.-S.; Cao, G.; Matsushima, T. *J. Phys. Chem. B* **2004**, 108, 14232.
- (14) Turner, D. W.; Baker, C.; Baker, A. D.; Brundle, C. R. In *Molecular Photoelectron Spectroscopy*; John Wiley & Sons: London 1970; Chapter 3.